Int. J. Multiphase Flow Vol. 13, No. 2, pp. 145–159, 1987
Printed in Great Britain.

0301-9322/87 $3.00 + 0.00

PHASE AND VELOCITY DISTRIBUTIONS AND HOLDUP IN HIGH-PRESSURE STEAM/WATER STRATIFIED FLOW IN A LARGE DIAMETER HORIZONTAL PIPE

M. KAWAJI,† Y. ANODA, H. NAKAMURA and T. TASAKA
Department of Reactor Safety Research, Japan Atomic Energy Research Institute, Tokai-mura, Ibaraki-ken, Japan

(*Received* 17 *October* 1985; *in revised form* 15 *July* 1986)

Abstract—High-pressure (3–12 MPa) steam/water two-phase flow in a 180 mm i.d. horizontal pipe has been experimentally investigated with emphasis on the study of phase and velocity distributions and liquid holdup. The phase and velocity distributions measured along the vertical centerline of the pipe indicate clear separation of the phases across the wavy interface region. The dimensionless velocity profiles in the liquid phase follow the logarithmic distribution near the bottom of the pipe, but deviate away close to the wavy interface due to interfacial shear. The liquid holdup data can be satisfactorily correlated using a Martinelli parameter for mass velocities $>200\ kg/m^2 s$. However, the condition at the outlet of the test section has a significant effect on holdup at mass velocities $<100\ kg/m^2 s$. When the water level in the tank, to which the test section discharges, is below the test section outlet, constant values of liquid holdup are obtained at low qualities which depend only on the liquid mass velocity. When the water level in the discharge tank is kept above the test section, the gravity head at the exit decelerates the liquid flow and significantly higher liquid holdup values are obtained. The holdup data at low mass velocities were correlated in terms of dimensionless flow rates for both cases.

1. INTRODUCTION

Horizontal two-phase flow has been studied in the past by many investigators, however, most of the experimental studies were conducted with low-pressure air/water systems in small diameter (typically 50 mm dia) tubes. There are many applications, particularly in the nuclear, chemical, petroleum and other industries where two-phase flows occur in much larger diameter pipes, and in some cases at elevated pressures. For example, the two-phase flow behavior in large diameter horizontal pipes is of importance in connection with the safety analysis of small-break loss-of-coolant accidents (LOCAs) in pressurized water reactors (PWRs), because of its effect on the decay heat removal from the reactor core.

In the past, few studies have addressed the two-phase flow in large diameter pipes. Simpson *et al.* (1981) identified the flow patterns and also measured the pressure drop and void fraction for air/water two-phase flows in 216 and 125 mm i.d. horizontal pipes at pressures close to atmospheric. For steam/water two-phase flow, Lester (1958) analyzed the pressure drop measurements obtained in 103 and 154 mm i.d. pipes at pressures up to 0.7 MPa. Harrison (1975) and Freeston (1979) analyzed the geothermal experimental data obtained in pipes of 200 and 100 mm i.d. at pressures up to 1.3 and 1.1 MPa, respectively. Reimann & John (1978) and Reimann *et al.* (1981) investigated the steam/water horizontal two-phase flow at pressures up to 10 MPa, but in 50 and 66 mm i.d. pipes.

There are no other published studies to our knowledge which have investigated steam/water two-phase flow in large diameter pipes at high pressures that are encountered in reactor accident conditions. The objectives of the present study are, therefore, to obtain and analyze the experimental data on horizontal two-phase flow of steam and water in large pipes at pressures up to 12 MPa. The data would be useful in developing or validating various correlations for prediction of liquid holdup, flow patterns and other two-phase flow parameters.

We will first describe the test facility including the two-phase flow instruments and then discuss the results of a series of experiments conducted with a large diameter horizontal pipe at pressures

†Present address: Department of Chemical Engineering and Applied Chemistry, University of Toronto, Toronto, Ontario M5S 1A4, Canada.

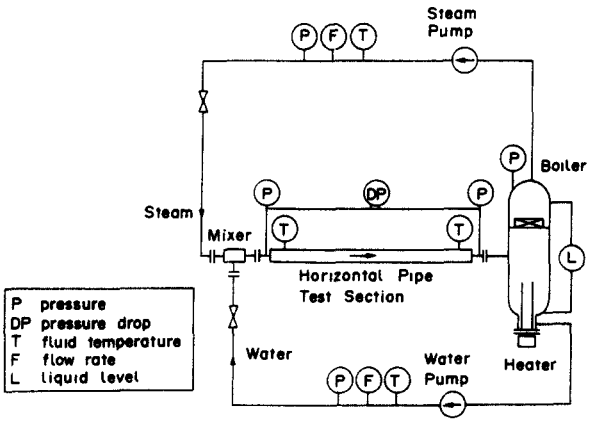

Figure 1. Test facility schematic.

up to 12 MPa. In this work, the phase and velocity distributions as well as holdup data for separated (stratified and wavy-stratified) flow patterns are presented and discussed.

2. TEST FACILITY AND INSTRUMENTATION

The experimental facility used in this work is the Two-phase Flow Test Facility (TPTF) constructed at the Japan Atomic Energy Research Institute's Tokai Establishment. This facility has been designed to perform various steam/water two-phase flow and heat-transfer experiments at steady state and at pressures up to 12.8 MPa.

The flow loop used in the present series of experiments is shown in figure 1 and consists of an electrically heated boiler, separate pumps for steam and water lines, a mixer and a 10 m long, 180 mm i.d. horizontal test section. The demineralized water is heated in the boiler to saturation conditions at a desired system pressure. Saturated steam is pumped from the top of the boiler through an orifice meter and into the mixer located at the entrance of the test section. The steam pump is a blower-type pump that was specially designed and manufactured for use at high pressure. The steam flows through a demister located at the top of the boiler and becomes slightly superheated at the exit of the pump. Saturated liquid is drawn from the bottom of the boiler and similarly pumped through an orifice meter into the mixer. The piping for both steam and liquid lines is well-insulated to minimize heat loss and prevent steam condensation or liquid subcooling.

The mixer is T-shaped as schematically shown in figure 2. The steam is introduced horizontally into a bundle of tubes and is forced out through numerous holes drilled along the side of each tube. Liquid introduced from the bottom of the tee flows on the outside of the tube bundle, where the steam and liquid mix with each other. A nearly homogeneous mixture of liquid and vapor is expected to enter the test section.

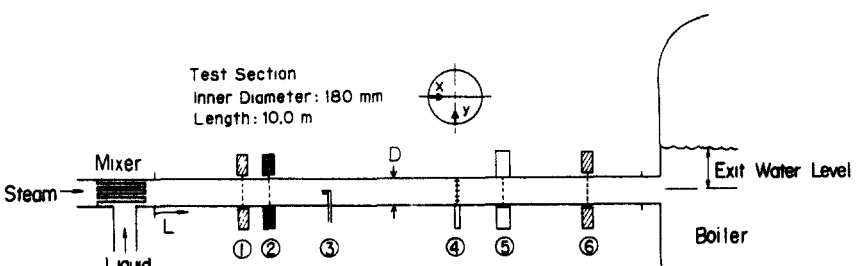

No	Instrument	Traversing Direction	Location (L/D)
1	γ- Densitometer	Horizontal	17
2	γ- Densitometer	Vertical	21
3	Pitot Tube	Vertical	25
4	Conduction Probe Rake	Fixed	36
5	γ- Densitometer	Fixed	40
6	γ- Densitometer	Horizontal	48

Figure 2. Test section and two-phase flow instrumentation.

The test section consists of five sections of 180 mm i.d. stainless-steel piping, each 2 m long and joined by Graylocs. The overall length is 10.0 m and the length-to-diameter ratio (L/D) is 56. The volumetric flow rates of vapor and liquid entering the test section can be changed independently by adjusting the flow control valves and the pump speed. The maximum volumetric flow rates are 0.194 m^3/s for steam and 0.047 m^3/s for liquid. For the 180 mm i.d. test section, the maximum superficial liquid and vapor velocities are 1.9 and 7.6 m/s, respectively. A complete description of the test facility is given by Nakamura *et al.* (1983).

The horizontal test section is equipped with various two-phase flow instruments, as shown in figure 2. In order to obtain detailed information about the flow structure, several of the instruments are attached to traversing devices which enable measurement of mass and momentum distributions across the pipe cross section. To measure density (or void) distribution, two of the γ-densitometers with vertically-shot γ-ray beams are traversed across the pipe cross section horizontally, yielding a horizontal distribution of vertical chord-average void fractions at locations near the inlet (L/D = 17) and outlet (L/D = 48) of the test section. The third densitometer with a horizontal beam is traversed vertically across the pipe cross section at L/D = 21, yielding a vertical distribution of horizontal chord-average void fractions. The fourth is a three-beam densitometer fixed to the pipe.

In every densitometer system, the γ-source is a 20 Ci, ^{137}Cs γ-emitter enclosed in a shielding cask. The beams are well-collimated and detected with NaI scintillation detectors, which are water-cooled to prevent temperature drift. For the traversing densitometers, the source and the detector assembly are installed on a platform and moved together horizontally or vertically across the pipe. The distance of each traversing step and the duration of counting can be changed to meet the desired level of spatial resolution and the statistical and dynamic errors.

From the detector signals, chord-average void fractions are calculated for each beam at each counting position using the log interpolation method. The intensities for the single-phase liquid and vapor conditions are obtained separately by conducting single-phase runs at the same pressure.

To measure momentum flux, a water-purged Pitot tube is used. The Pitot tube is attached to a driving mechanism which moves the probe vertically along the centerline of the pipe at a speed of 0.22 mm/s to measure the momentum flux distribution. The water-purge is necessary for use at high temperatures to prevent generation of voids in the pressure sensing lines. The subcooled purge-water is continuously supplied at a constant rate of 0.5 ml/s with two positive displacement pumps which are operated in tandem. Due to purging, the response of the Pitot tube is reduced in comparison with a non-purged Pitot tube. Therefore, the Pitot coefficient was determined by separately conducting calibration tests in a wind tunnel.

To further aid in flow pattern identificaton, five conductivity probes specially developed for use in high-temperature and high-pressure steam/water environments are attached to a rod which is situated along the vertical centerline of the test section. The fast response of the probes made discrimination between the separated and slug flows possible as described in the next section.

All of the instruments are connected to a multichannel data logger and sampled simultaneously at a rate of 5 Hz for 400 s in each run. During this sampling period, the traversing instruments complete a sweep across the pipe cross section from one end to the other. To mainly record the conductivity probe signals, a second sampling of all instruments is performed at 100 Hz for 20 s. The data collected were processed by an off-line computer.

3. TEST CONDITIONS AND FLOW PATTERN IDENTIFICATION

The parameters that were varied in the present series of experiments include the system pressure (and the corresponding saturation temperature), inlet mass flux and flow quality as listed in table 1. In addition, the effect of the test section exit conditions was investigated by setting the water level in the boiler, to which the test section discharges, either above or below the test section exit.

Investigation of the effect of the exit conditions was motivated by the consideration of the geometries of the hot-leg and cold-leg piping in the PWRs. The hot leg connects the reactor vessel's upper plenum to the inlet plenum of the steam generator, and the cold leg conects the primary coolant pump discharge to the reactor vessel downcomer. The conditions at the exit of the hot leg may vary depending on whether or not the coolant remains in the steam generator inlet plenum during a small-break LOCA. If the steam generator inlet plenum is filled with the coolant, there

Table 1. Range of experimental conditions

Pressure (temperature)	3.0 MPa (234°C) 7.5 MPa (291°C) 12.0 MPa (325°C)
Flow rate	
G: mass velocity	0–1000 kg/m^2 s
x: quality	0.003–0.90
Test section	180.0 mm i.d., 10.0 m long

is likely to be a gravity head effect on the two-phase flow in the hot leg. Similarly, the coolant level in the downcomer would affect the flow in the cold leg.

The experiments were performed at a specified pressure under steady, saturation conditions. The flow rate of each phase was independently adjusted and brought to a steady state before recording the data. In the present work, only the separated flow (stratified and wavy–stratified) data will be presented and discussed, since this was the only flow pattern observed using the bubbly flow mixer (well-mixed inlet conditions) described above. Slug flow was observed, however, when a "separated mixer" was used that contains a flat plate and delivers the two phases into the test section completely separated. Identification of the separated and slug flow patterns was initially made quite unambiguously by examining the temporal variations in the densitometer, Pitot tube and conduction probe signals. The characteristics of the instrument signals under the stratified and slug flow patterns were later verified by directly looking into the pipe with an optical probe designed for use at high pressure. Typical flow patterns were recorded with a TV camera connected to a video recorder.

The effect of the inlet conditions on the flow pattern described above may be attributed to the relatively short test section (180 mm i.d., 10 m long) involved. The L/D ratio of the present test section (56) may be considered too small to obtain well-developed two-phase flows, and transition from stratified to slug flow may eventually take place in certain cases, if the test section were much longer.

As will be discussed shortly, the vertical void fraction profile measurements at 3.8 m (L/D = 21) from the test section inlet indicated clear separation of phases after the two-phase mixture enters the test section through the bubbly flow mixer. Other measurements downstream further indicated that the phases remain separated throughout the test section. Although the separated flow data discussed in this paper may not be representative of well-developed flows, the results should be of considerable interest to reactor safety applications, because the L/D ratios of the hot and cold legs of PWRs are even smaller than that of our test section.

4. PHASE AND VELOCITY DISTRIBUTIONS

Typical void (or liquid) fraction and momentum flux profiles obtained for separated flow pattern are shown in figures 3 and 4. The horizontal liquid fraction distributions, measured at L/D = 17

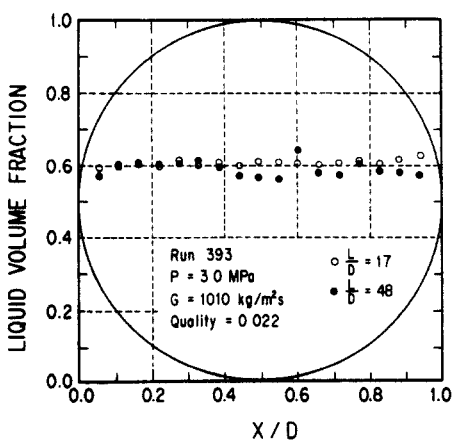

Figure 3. Liquid fraction distributions measured at L/D = 17 and 48.

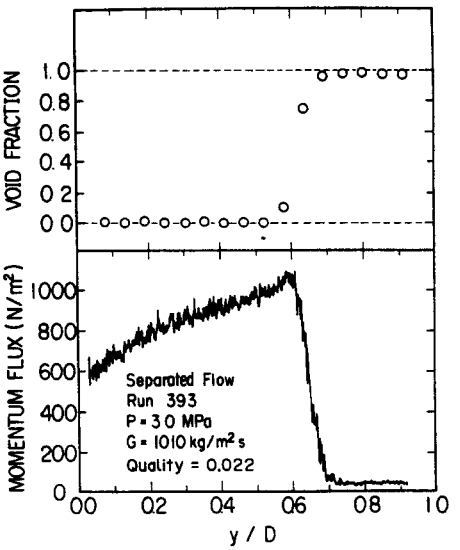

Figure 4. Chord-average void fraction and momentum flux distributions along the vertical centerline of the pipe (y measured from the bottom of the pipe).

and 48 and shown in figure 3, indicate a flat but somewhat irregular liquid–vapor interface. The vertical void and momentum flux distributions measured along the centerline of the pipe are seriated as expected.

The vertical void fraction profile measured at L/D = 21 indicates the presence of interfacial waves. The void fraction increases sharply across the vapor–liquid interface, but over a region of finite amplitude. The higher the wave amplitude, the less sharply the void fraction varies near the interface. The interfacial waves grow in amplitude as they travel further downstream and the liquid–vapor interface becomes highly turbulent and irregular as can be observed from a comparison of the horizontal liquid fraction distributions measured at L/D = 17 and 48.

The momentum flux measured at L/D = 25, and shown in figure 4, increases steadily from the bottom of the pipe upward, reaches a peak and then rapidly drops and remains at a lower value in the upper part of the pipe. The peak in the momentum flux profile is observed to occur near the collapsed liquid level measured at L/D = 17, shown in figure 3. The rapid drop in momentum flux near the interface region is due to the sudden change in fluid density across the wavy interface.

Measurement of the velocity distributions in separated flow (stratified and wavy flows) is useful for understanding of the interphase momentum transfer mechanism and development of an interfacial shear correlation needed in two-fluid models. Previous studies on velocity profiles and turbulence structure have been conducted in mainly low-pressure air/water or steam/water systems for cocurrent separated flows (Jensen & Yuen 1982; Fabre *et al.* 1984) and in open-channel liquid flows (Nalluri & Novak 1973; Ueda *et al.* 1977).

To obtain the local velocity from the momentum flux measurements, the local void fraction must be known at the same measurement location. The horizontal and vertical void fraction distributions for a separated flow obtained with the traversing γ-densitometers indicate that the single-phase liquid or vapor can be assumed in regions above or below the wavy interface region, respectively. Furthermore, by comparing the momentum flux and void fraction profiles such as those shown in figure 4, the time-averaged boundaries of the wavy interface region can be estimated quite accurately.

In two-phase flow, one must further consider the momentum exchange factor when calculating velocity from the Pitot tube data (Reimann 1983). The momentum exchange factor is given as a function of void fraction and has a value between 1 and 2, however, the models suggested in the past vary quite widely from one another (Kastner *et al.* 1985). Thus, in the present work the velocity profiles were calculated from the momentum flux data only in regions above and below the wavy interface with the single-phase vapor and liquid densities respectively, and with the momentum exchange factor of unity for both cases.

Table 2. Experimental conditions for velocity measurement

Run	P (MPa)	U_{SL} (m/s)	U_{SG} (m/s)
354	3.0	0.39	5.49
360	3.0	1.11	6.85
365	3.0	1.22	0.68
371	3.0	1.17	0.35
373	3.0	1.17	3.43
743	7.3	1.10	5.10
747	7.4	1.27	2.02
749	7.4	1.31	1.28
751	7.4	1.35	0.51
753	7.4	1.36	0.26
1247	11.8	0.92	5.73
1292	11.7	1.38	1.46

The velocity profiles obtained at 7.5 MPa for the flow rates given in table 2 are shown in figure 5. The wavy interface region is indicated by a shaded area. As the vapor flow rate is increased for nearly the same liquid flow rate, the position of the wavy liquid–vapor interface is lowered and the average liquid velocity increases. The amplitude of the wavy region is seen to increase with increasing vapor flow rate. The plane of maximum vapor velocity can be identified in most cases except when the interfacial wave amplitude becomes rather large.

The velocity profiles in the liquid phase can be examined in greater detail by plotting the data in non-dimensional form, as shown in figure 6. The momentum flux distributions were measured at pressures of 3, 7.5 and 12 MPa with the steam and water flow rates given in table 2. The velocity, U_L, and distance, y, measured from the bottom of the pipe vertically upward along the centerline, are made dimensionless with a scaling velocity, U^*:

$$U_L^+ = \frac{U_L}{U^*} \quad [1]$$

$$y^+ = \frac{yU^*}{\nu_L}. \quad [2]$$

Here, ν_L is the kinematic viscosity of the liquid. The scaling velocity, U^*, is closely related to the wall–liquid friction velocity, however, for the data presented in figure 6, the values of U^* were chosen so as to match the measured dimensionless velocity with the universal velocity distribution given below, at a value of $y^+ = 10^4$:

$$U_L^+ = 2.5 \ln y^+ + 5.5. \quad [3]$$

It is noted here that the large values of y^+ obtained in this study in comparison with those in low-pressure air/water flows in small diameter tubes are mainly due to the reduction in liquid viscosity at high temperatures and pressures, and the large diameter of the present test section.

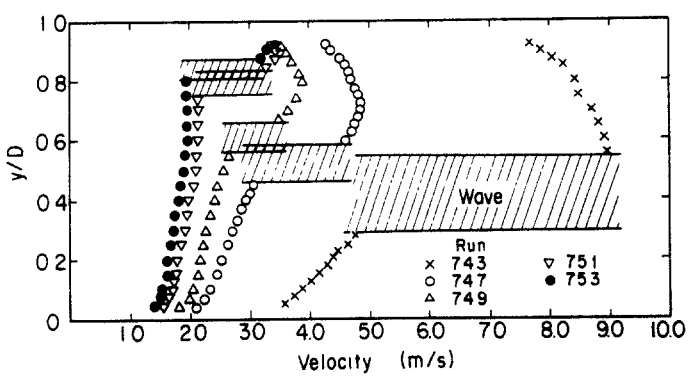

Figure 5. Velocity distributions along the vertical centerline of the pipe (pressure = 7.5 MPa, L/D = 25).

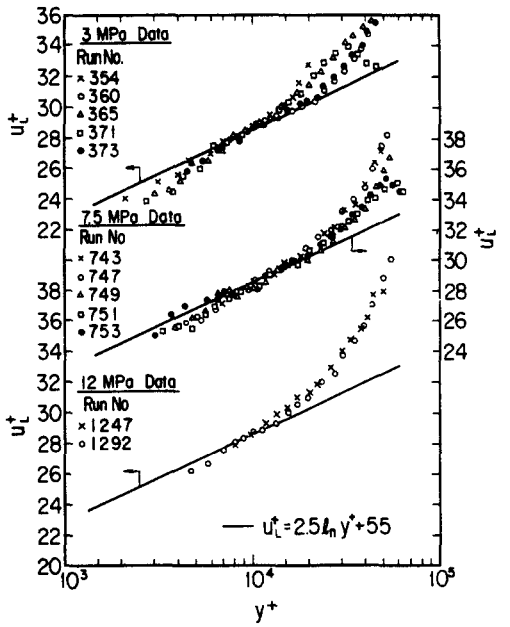

Figure 6. Non-dimensionalized velocity profiles in the liquid phase.

The velocity profiles measured in the liquid phase are observed to follow the curve given by [3] at all pressures in the fully-turbulent region at the bottom of the pipe, where $y^+ \lesssim 1.5 \times 10^4$. As the liquid–vapor interface is approached and y^+ exceeds 1.5×10^4, the velocity gradient changes and velocity increases in most cases deviating away from the universal distribution curve.

In calculating the velocity from the momentum flux data, the single-phase liquid density was used below the wavy interface region. The actual density near the interface may be slightly less than the liquid density due possibly to the vapor entrainment. As a result, the liquid velocities just below the interface may have been underestimated. This does not, however, affect the observations on liquid velocity profile given above.

The scaling velocity, U^*, was found to be closely related to the friction velocity evaluated from the wall–liquid shear stress,

$$U_{WL} = \sqrt{\frac{\tau_{WL}}{\rho_L}}, \qquad [4]$$

where the wall–liquid shear, τ_{WL}, was calculated with the average liquid velocity, U_L, and a friction factor, f_{WL}:

$$\tau_{WL} = \frac{f_{WL}\rho_L U_L^2}{2} \qquad [5]$$

$$f_{WL} = 0.046\,\mathrm{Re}^{-0.2}. \qquad [6]$$

The Reynolds number is computed with the hydraulic diameter for liquid which is defined in terms of the wetted perimeter of the pipe, S_L, and the flow area occupied by the liquid phase, A_L:

$$\mathrm{Re} = \frac{U_L D_{EL}}{\nu_L} \qquad [7]$$

$$D_{EL} = \frac{4A_L}{S_L} \qquad [8]$$

As shown in figure 7, the scaling velocity, U^*, matches the wall–liquid friction velocity, U_{WL}, quite well. The present results, thus, indicate that at all pressures, the liquid flow in the lower layer close to the bottom wall is similar to that in fully turbulent single-phase flow in a tube, but the flow in the upper layer close to the interface is strongly affected by the interfacial shear.

Similar results for the liquid velocity profiles have been reported for low-pressure air/water open-channel flow by Nalluri & Novak (1973) and Ueda *et al.* (1977) among others, and for

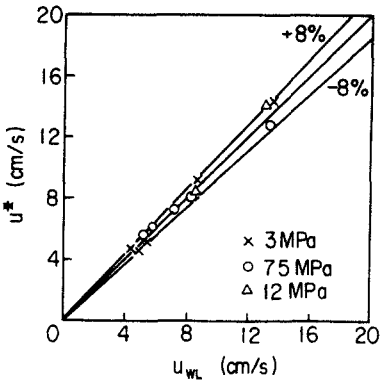

Figure 7. Comparison of scaling velocity and friction velocity.

cocurrent stratified flow by Jeffries *et al.* (1969) and more recently by Fabre *et al.* (1984). Furthermore, Fabre *et al.* (1984) have proposed, based on their measurements, a two-layer model to describe the flow in the liquid phase. In the lower layer, the eddy viscosity concept is applicable and the liquid velocity profile is fit with a logarithmic law just as in our case. In the upper layer, turbulence generated at the liquid–vapor interface due to the interfacial waves predominates and the length and velocity scales needed are linked to the interfacial wave structure.

5. PHASE HOLDUP

The liquid holdup in a horizontal pipe is an important parameter for prediction of two-phase pressure drop, flow pattern transition etc. It is also important for reactor safety applications, since the liquid holdup in the large diameter horizontal piping of a PWR primary loop significantly affects the break flow rate when a small break occurs at the side or bottom of the main pipe (Reimann & Khan 1984).

The liquid holdup in the present study is defined as the cross-sectional area-averaged liquid fraction, α_L, which is equal to $1-\alpha_G$, where α_G is the area-averaged void fraction obtained by weighted-averaging of chord-average void fractions measured with the traversing γ-densitometers. The weighted-averaging is performed with the chord length as the weighting factors. In the case of stratified and wavy flows, the liquid holdup can also be estimated from the vertical void fraction profiles by locating the average position of the liquid–vapor interface.

The liquid holdup in cocurrent horizontal two-phase flow has been extensively studied in the past. Lockhart & Martinelli (1949) first attempted to correlate their adiabatic, low-pressure air/water data in terms of the parameter, X, where $X^2=(\mathrm{d}P/\mathrm{d}x)_{LO}/(\mathrm{d}P/\mathrm{d}x)_{GO}$ is the ratio of the frictional pressure gradient of the liquid to that of the gas when each phase flows alone in the pipe. Several other correlations have later been published, but Butterworth (1975) has shown that the correlations of Lockhart & Martinelli (1949), Zivi (1963), Turner & Wallis (1965), Thom (1964) and Baroczy (1963) are essentially of the form

$$\frac{\alpha_L}{1-\alpha_L}=A\left(\frac{1-x}{x}\right)^p\left(\frac{\rho_G}{\rho_L}\right)^q\left(\frac{\mu_L}{\mu_G}\right)^r, \qquad [9]$$

where x denotes quality, ρ is density and μ is the viscosity of the fluid. The coefficients, A, p, q, and r, have values between 0 and 1.0 depending on the specific correlation. Chen & Spedding (1983) have additionally shown that the drift flux formulation of Zuber & Findlay (1965) can also be arranged in a manner similar to [9] but with extra terms added to the r.h.s.

Common to all of the correlations mentioned above is the absence of terms accounting for the effect of flow pattern and mass velocity. Johannessen (1972), Taitel & Dukler (1976) and more recently Chen & Spedding (1981) have shown that there is a theoretical basis for correlating the holdup data in stratified and annular flows in terms of the Martinelli parameter, X. For the case of stratified flow, the Martinelli parameter can be computed from quality and physical properties of gas and liquid, and does not depend on the mass velocity for turbulent flow regimes in both

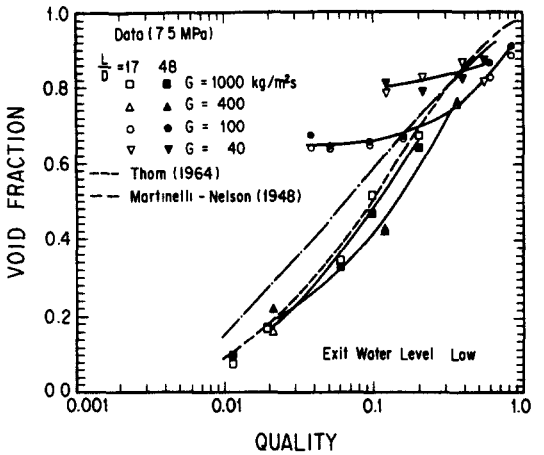

Figure 8. Variation of void fraction with quality for different mass velocities (case of low exit water level, $P = 7.5$ MPa).

phases:

$$X_{tt} = \left(\frac{\rho_G}{\rho_L}\right)^{0.5} \left(\frac{1-x}{x}\right)^{0.9} \left(\frac{\mu_L}{\mu_G}\right)^{0.1}. \qquad [10]$$

The area-averaged void fraction data obtained in the present study at a pressure of 7.5 MPa are shown in figure 8 and listed in table 3. The data shown were measured at L/D = 17 and 48 with the bubbly flow mixer at the inlet. The water level in the boiler, to which the test section discharges, was kept well below the test section exit in all runs. This outlet condition is referred to as the low exit water level case. Also shown in figure 8 are the correlations of Martinelli & Nelson (1948) and Thom (1964), both of which are applicable to high-pressure steam/water systems.

There is little difference between the holdup values obtained at L/D = 17 and 48 for a given mass velocity and inlet quality. Although the two phases are well mixed at the inlet, they tend to separate quickly due to gravity and flow downstream without a significant change in void fraction. At mass velocities >400 kg/m^2 s, the void fraction decreases steadily with diminishing quality and is well-predicted by the Thom correlation. A strong mass velocity effect is evident, however, for low mass velocity/low quality flow conditions. At mass velocities <100 kg/m^2 s, the void fractions coincide with those of high mass velocity only at high quality, but asymptotically reach constant

Table 3. Holdup values measured for low exit water level

Run	P (MPa)	G (kg/m^2 s)	x	U_{SL} (m/s)	U_{SG} (m/s)	Void fraction L/D = 17	Void fraction L/D = 48
857	7.4	1016	0.200	1.12	5.15	0.67	0.64
855	7.4	1020	0.104	1.26	2.69	0.51	0.47
853	7.4	1025	0.060	1.33	1.55	0.35	0.33
851	7.4	1015	0.020	1.37	0.52	0.17	0.17
849	7.4	1015	0.011	1.38	0.28	0.08	0.10
845	7.4	440	0.374	0.38	4.17	0.76	0.77
843	7.4	442	0.122	0.54	1.37	0.42	0.42
847	7.4	426	0.022	0.57	0.23	0.16	0.22
836	7.5	114	0.810	0.030	2.33	0.89	0.91
838	7.4	112	0.634	0.056	1.79	0.83	0.87
1561	7.6	116	0.153	0.14	0.45	0.67	0.68
1563	7.6	114	0.093	0.14	0.27	0.65	0.66
1565	7.6	115	0.052	0.15	0.15	0.64	0.65
1567	7.7	116	0.038	0.16	0.11	0.64	0.67
834	7.5	42.6	0.575	0.025	0.62	0.82	0.88
1555	8.0	45.2	0.378	0.041	0.42	0.87	0.83
1557	7.8	43.5	0.209	0.049	0.23	0.83	0.79
1559	7.7	42.8	0.122	0.053	0.13	0.79	0.82

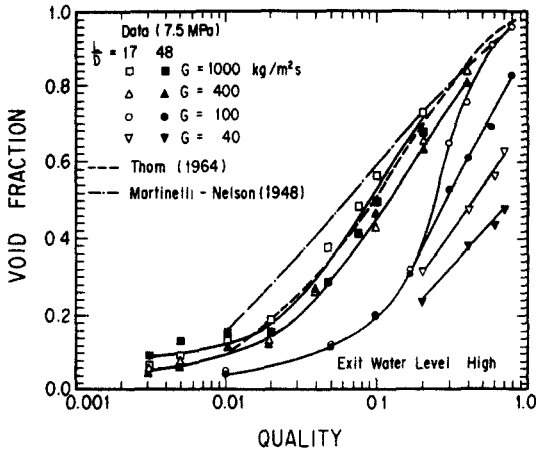

Figure 9. Variation of void fraction with quality for different mass velocities (case of high exit water level, $P = 7.5$ MPa).

values at lower quality. The asymptotic values are clearly dependent on the mass velocity. Similar trends in the holdup data for stratified flow have been reported by Chen & Spedding (1984) for low pressure, air/water experiments using a 45.5 mm i.d. pipe and by Simpson *et al.* (1981) for both 127 and 216 mm i.d. pipes.

The effect of exit conditions was also studied by measuring the holdup with the water level in the boiler raised to a level about 0.4 m above the center of the test section exit. The area-averaged void fraction data obtained at L/D = 17 and 48 for this high exit water level case are shown in figure 9 and listed in table 4. The void fraction data obtained at high mass velocities show little difference from those for the low exit water level case and are again well-represented by the Thom correlation. However, at low mass velocities, the void fraction decreases with a reduction in mass velocity in contrast with the low exit water level case. The void fraction also decreases (or liquid

Table 4. Holdup values measured for high exit water level

Run	P (MPa)	G (kg/m² s)	x	U_{SL} (m/s)	U_{SG} (m/s)	Void fraction L/D = 17	Void fraction L/D = 48
779	7.3	1011	0.0030	1.38	0.085	0.06	0.09
781	7.3	1013	0.0050	1.37	0.13	0.09	0.13
775	7.3	1010	0.010	1.37	0.26	0.13	0.15
751	7.4	1007	0.019	1.35	0.51	0.19	0.15
749	7.4	1004	0.048	1.31	1.28	0.38	0.29
747	7.4	1001	0.077	1.27	2.02	0.48	0.41
773	7.3	1010	0.101	1.24	2.58	0.57	0.50
743	7.4	1000	0.195	1.10	5.10	0.73	0.69
732	7.4	400	0.391	0.33	4.10	0.84	0.81
730	7.3	402	0.196	0.44	2.06	0.66	0.64
783	7.3	414	0.106	0.51	1.11	0.43	0.47
785	7.3	410	0.039	0.54	0.41	0.26	0.27
755	7.4	407	0.019	0.55	0.21	0.13	0.13
757	7.4	383	0.010	0.52	0.10	0.16	0.12
759	7.4	381	0.0050	0.52	0.050	0.08	0.06
761	7.4	380	0.0030	0.52	0.031	0.06	0.04
726	7.4	99.1	0.794	0.028	2.06	0.97	0.83
728	7.3	100	0.596	0.055	1.57	0.91	0.69
708	7.3	99.4	0.293	0.10	0.76	0.65	0.53
710	7.3	99.5	0.391	0.083	1.02	0.76	0.61
1545	7.4	106	0.164	0.12	0.44	0.32	0.31
1547	7.4	103	0.098	0.13	0.26	0.20	0.20
1549	7.4	105	0.050	0.14	0.13	0.12	0.11
763	7.4	102	0.010	0.14	0.027	0.05	0.04
720	7.3	39.6	0.691	0.017	0.72	0.63	0.48
722	7.3	39.7	0.590	0.022	0.61	0.57	0.44
712	7.3	39.9	0.392	0.033	0.41	0.48	0.38
714	7.3	40.2	0.196	0.044	0.21	0.31	0.24

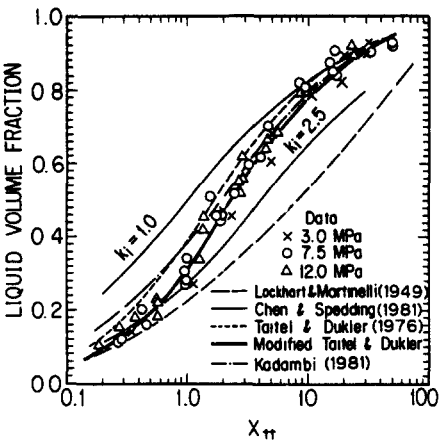

Figure 10. Correlation of liquid holdup data for separated flow at high mass velocities ($200\ kg/m^2\ s < G < 1000\ kg/m^2\ s$).

holdup increases) more significantly at the downstream end (L/D = 48) for low mass velocity, high quality flows.

The exit effect observed can be explained in qualitative terms as follows. The higher water level in the boiler presents an increased resistance at the test section exit due to the gravity head proportional to the elevation of the collapsed water level in the boiler relative to the test section. This added resistance at the exit decelerates the liquid flow and from consideration of continuity, causes an increase in liquid holdup. The corresponding decrease in void fraction and increase in both vapor velocity and relative velocity between the two phases, results in increased interfacial shear and a new equilibrium interface level is reached. Thus, the conditions at the test section exit, namely the water level relative to the test section, are found to have a pronounced effect on liquid holdup for stratified flow of mass velocity $< 100\ kg/m^2\ s$, but little effect at mass velocities $> 400\ kg/m^2\ s$.

6. CORRELATION OF THE HOLDUP DATA

The holdup data described above are analyzed in this section. In order to represent the average holdup in the test section, arithmetic averages of the holdup values obtained at L/D = 17 and 48 are computed and either correlated or compared with the existing correlations.

Mass velocity $> 200\ kg/m^2\ s$

The liquid volume fraction data for mass velocity $\gtrsim 200\ kg/m^2\ s$ obtained at pressures of 3, 7.5 and 12 MPa are shown in figure 10 with the Martinelli parameter computed using [10]. Also shown in figure 10 are the correlations of Taitel & Dukler (1976), Lockhart & Martinelli (1949), Kadambi (1981) and Chen & Spedding (1981). Data for the boiler water level both higher and lower than the test section exit are included in the figure. Both the Kadambi (1981) and Taitel & Dukler (1976) correlations were developed specifically for the stratified flow geometry, and are found to only slightly overpredict the present data. The correlation proposed by Chen & Spedding (1981),

$$\alpha_L = \frac{X_{tt}^{2/3}}{k_i + X_{tt}^{2/3}} \qquad [11]$$

with $k_i = 1.0$ and 2.5, describes the boundaries of the present data. The value of k_i is believed to be dependent on the pipe size and a value of 2.5 was recommended for a 20 cm pipe. The Lockhart & Martinelli (1949) correlation was developed from low-pressure data and significantly underpredicts the present data.

The best fit of the above data was obtained, as described below, by slightly modifying the method that Taitel & Dukler (1976) used to derive their correlation. Taitel & Dukler (1976) assumed an equal friction coefficient for calculation of interfacial and vapor–wall shear stresses. However, in the present experiments, the vapor–liquid interface is observed to be considerably disturbed at high

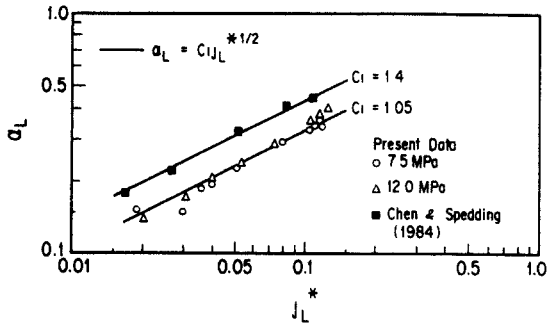

Figure 11. Correlation of liquid holdup data for low mass velocity and low exit water level (separated flow, $G < 100\,kg/m^2\,s$).

mass velocity conditions, as evident from the vertical void fraction distribution data. Thus, we calculated the liquid holdup for different values of X_{tt}, assuming the interfacial friction to be greater than the vapor–wall friction by some constant factor. As shown by the solid curve in figure 10, the best fit of the present data was obtained for the constant factor of 3. The curve is seen to fit the void fraction data for the present range of high mass velocity better than the original Taitel & Dukler (1976) correlation.

Mass velocity $< 100\,kg/m^2\,s$

The holdup data for mass velocity $< 100\,kg/m^2\,s$ show distinctly different behavior from those at higher mass velocities and can not be predicted by any of the correlations which are based on the Martinelli parameter. In addition, the holdup behavior is completely different depending on the conditions at the discharge end of the test section, as described previously.

For the case of the boiler water level kept below the test section exit, the vapor holdup reaches a constant value at low mass velocity and low quality conditions. The asymptotic value of the void fraction depends mainly on the liquid flow rate, and the vapor flow rate has little effect. This suggests conditions similar to a free discharge of liquid from a horizontal pipe. In open-channel flows, a Froude number is often used to correlate the flow parameters, and its use was considered for prediction of the liquid holdup data under low mass velocity/low quality conditions. The holdup data are plotted in figure 11 against the dimensionless liquid flux, $j_L^* = \rho_L^{0.5} U_{SL}/[gD(\rho_L - \rho_G)]^{0.5}$, which is essentially a Froude number for two-phase flow. Here, U_{SL} is the superficial liquid velocity. The data obtained at pressures of 7.5 and 12.0 MPa and listed in tables 3 and 5 for low mass velocity ($U_{SL} + U_{SG} < 1.5$ m/s) can be well-correlated by the following equation:

$$\alpha_L = 1.05 j_L^{*1/2}. \quad [12]$$

The holdup data reported by Chen & Spedding (1984) are also shown in figure 11 and are seen to similarly vary linearly with the square root of j_L^*.

For the case of the boiler water level kept above the test section exit, the void fraction is substantially reduced as the mass velocity decreases. The vapor holdup can not be predicted in

Table 5. Additional holdup values for low exit water level

Run	P (MPa)	G (kg/m² s)	x	U_{SL} (m/s)	U_{SG} (m/s)	Void fraction L/D = 17	Void fraction L/D = 48
1581	11.6	101	0.395	0.092	0.57	0.32	0.26
1601	11.8	106	0.193	0.13	0.30	0.39	0.34
1603	11.8	105	0.107	0.14	0.16	0.42	0.36
1600	11.8	105	0.0	0.16	0.0	0.44	0.38
1596	11.7	41.2	0.588	0.026	0.35	0.15	0.13
1597	11.7	41.9	0.397	0.039	0.24	0.20	0.15
1598	11.8	42.8	0.228	0.050	0.14	0.23	0.18
1599	11.8	43.7	0.0	0.067	0.0	0.27	0.21
867	7.7	84.9	0.120	0.10	0.26	0.31	0.28
868	7.8	60.5	0.180	0.070	0.27	0.24	0.22

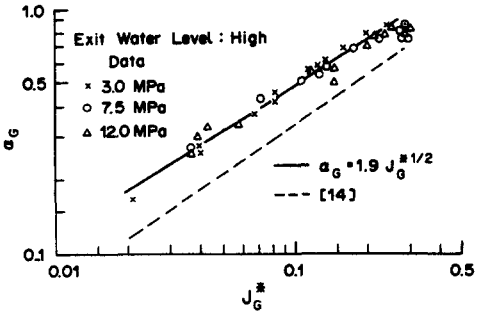

Figure 12. Correlation of liquid holdup data for low mass velocity and high exit water level (separated flow, $G < 100\ \text{kg/m}^2\,\text{s}$).

terms of the Martinelli parameter for the following reason. As the liquid flow rate approaches zero, the frictional pressure drop of the liquid phase diminishes and the Martinelli parameter decreases to a value of zero for any vapor flow rate. The existing correlations based on the Martinelli parameter predict zero liquid holdup (or void fraction of unity) for this limiting condition, however, the liquid holdup measured for no liquid flow conditions was found to remain finite and vary with the vapor flow rate.

Thus, the void fraction data for the low mass velocity/high exit water level case are plotted in figure 12 against the dimensionless vapor flux, $j_G^* = \rho_G^{0.5} U_{SG}/[gD(\rho_L - \rho_G)]^{0.5}$, which is proportional to the superficial vapor velocity, U_{SG}. The data obtained at pressures of 3, 7.5 and 12 MPa, and for low mass velocity ($j_L^* < 0.1$) can be well-correlated by the following equation:

$$\alpha_G = 1.9 j_G^{*1/2}. \qquad [13]$$

Equation [13] is strictly valid for the case of the boiler water level at the discharge end kept at about 0.4 m above the test section axis. The effect of increasing the boiler water level above 0.4 m could not be assessed due to facility limitations.

It is interesting to note here that [13] is quite similar in form to the correlation for the stability limit of separated flow in a horizontal channel proposed by Wallis & Dodson (1973), which can be expressed as follows:

$$\alpha_G = 1.6 j_G^{*2/3}. \qquad [14]$$

Separated–slug flow transition is predicted to occur when the void fraction is less than the critical value given by the r.h.s. of [14]. As shown in figure 12, the void fraction given by [13] for a given vapor flow rate is always greater than the critical value for the onset of slug flow predicted by [14]. This is consistent with the fact that both the void fraction data shown in figure 12 and [13] are for separated flow.

7. CONCLUSION

The void fraction and momentum flux profiles have been measured and analyzed for steam/water separated (stratified and wavy) flows at pressures between 3 and 12 MPa in a 180 mm i.d. horizontal pipe. In general, the void fraction profile in separated flow is horizontally symmetrical but vertically seriated as expected. The dimensionless velocity profile in the liquid layer closely follows the logarithmic distribution near the bottom of the pipe, however, closer to the wavy interface, the velocity is strongly affected by the interfacial shear.

The phase holdup was measured and correlated for mass velocities of up to $1000\ \text{kg/m}^2\,\text{s}$ at pressures between 3 and 12 MPa. At mass velocities $> 200\ \text{kg/m}^2\,\text{s}$, the holdup data can be well-correlated in terms of the Martinelli parameter. We have modified the Taitel & Dukler (1976) approach in order to obtain the best fit of the present data based on the observation of the enhanced interfacial shear due to the presence of interfacial waves.

For low mass velocities ($< 100\ \text{kg/m}^2\,\text{s}$), the holdup behavior is quite different from that of the higher mass velocity case. In addition, the holdup is strongly affected by the conditions at the discharge end of the test section. For the boiler water level kept below the test section exit, the liquid

holdup reached constant values at low qualities unaffected by the vapor flow rate. Based on a similarity with the open discharge flow, the liquid holdup data for low mass velocities ($U_{SL} + U_{SG} < 1.5$ m/s) were correlated in terms of the dimensionless liquid flux, j_L^*. For the opposite case, namely the boiler water level kept at about 0.4 m above the test section exit, the liquid holdup decreased with the increase in the vapor flow rate. In this case, the void fraction data for $j_L^* < 0.1$ were successfully correlated in terms of the dimensionless vapor flux, j_G^*.

REFERENCES

BAROCZY, C. J. 1963 Correlation of liquid fraction in two-phase flow with application to liquid metals. Report NAA-SR-8171.

BUTTERWORTH, D. 1975 A comparison of some void-fraction relationships for co-current gas–liquid flow. *Int. J. Multiphase Flow* **1**, 845–850.

CHEN, J. J. J. & SPEDDING, P. L. 1981 An extension of the Lockhart–Martinelli theory of two-phase pressure and holdup. *Int. J. Multiphase Flow* **7**, 659–679.

CHEN, J. J. J. & SPEDDING, P. L. 1983 An analysis of holdup in horizontal two-phase gas–liquid flow. *Int. J. Multiphase Flow* **9**, 147–159.

CHEN, J. J. J. & SPEDDING, P. L. 1984 Holdup in horizontal gas–liquid flow. In *Multi-phase Flow and Heat Transfer*; Vol. III, Part A: *Fundamentals* (Edited by VEZIROGLU, T. N. & BERGLES, A. E.), pp. 333–351. Elsevier, Amsterdam.

FABRE, J., MASBERNAT, L. & SUZZANE, C. 1984 Some remarks on the constitutive equations of stratified gas–liquid flow. In *Multi-phase Flow and Heat Transfer*; Vol. III, Part A: *Fundamentals* (Edited by VEZIROGLU, T. N. & BERGLES, A. E.), pp. 41–57. Elsevier, Amsterdam.

FREESTON, D. H. 1979 Duct losses in a geothermal steam water flow. In *Two-phase Momentum, Heat and Mass Transfer in Chemical, Process, and Energy Engineering Systems*, Vol. 2 (Edited by DURST, F., TSIKLAURI, G. V. & AFGAN, N.H.), pp. 603–615. Hemisphere, Washington, D.C.

HARRISON, R. F. 1975 Methods for the analysis of geothermal two-phase flow. Master's Thesis, School of Engineering, Univ. of Auckland, New Zealand.

JEFFRIES, R. B., SCOTT, D. S. & RHODES, E. 1969 Structure of turbulence close to the interface in the liquid phase of a cocurrent stratified two-phase flow. Paper 25. *Proc. Instn mech. Engng* **184** (3C), 204–214.

JENSEN, R. J. & YUEN, M. C. 1982 Interphase transport in horizontal stratified cocurrent flow. Report NUREG/CR-2334.

JOHANNESSEN, T. 1972 A theoretical solution of the Lockhart–Martinelli flow model for calculating two-phase flow pressure drop and holdup. *Int. J. Heat Mass Transfer* **15**, 1443–1449.

KADAMBI, V. 1981 Void fraction and pressure drop in two-phase stratified flow. *Can. J. chem. Engng* **59**, 584–589.

KASTNER, W., KEFER, V. & MANZANO-RUIZ, J. J. 1985 Applications of Pitot-meter techniques in two-phase, steam–water flow. In *Fundamental Aspects of Gas–Liquid Flows* (Edited by MICHAELIDES, E. E.); *ASME FED*, Vol. 29, pp. 47–52.

LESTER, G. W. 1958 Correlation of two-phase pressure-drop measurements for steam–water mixtures in a 4.06″ diameter and a 6.06″ diameter horizontal pipeline. Report AERE CE/M 217.

LOCKHART, R. W. & MARTINELLI, R. C. 1949 Proposed correlation of data for isothermal two-phase, two-component flow in pipes. *Chem. Engng Prog.* **45**, 39–48.

MARTINELLI, R. C. & NELSON, D. B. 1948 Prediction of pressure drop during forced circulation boiling of water. *Trans. ASME* **70**, 695–702.

NAKAMURA, H., TANAKA, H., TASAKA, K., KOIZUMI, Y. & MURATA, H. 1983 System description for ROSA-VI two-phase flow test facility (TPTF). Report JAERI-M-83-042.

NALLURI, C. & NOVAK, P. 1973 Turbulence characteristics in a smooth open channel of circular cross section. *J. hydraul. Res.* No. 4, 343–368.

REIMANN, J. 1983 Developments in two-phase mass flow rate instrumentation. In *Advances in Two-phase Flow and Heat Transfer, Fundamentals and Applications*, Vol. 1 (Edited by KAKAC, S. & ISHII, M.), pp. 339–402. Martinus Nijhoff, Boston, Mass.

REIMANN, J. & JOHN, H. 1978 Measurements of the phase distribution in horizontal air–water

and steam–water flow. In *Proc. 2nd CSNI Specialist Mtg on Transient Two-phase Flow*, Paris, pp. 613–626.

REIMANN, J. & KHAN, M. 1984 Flow through a small break at the bottom of a large pipe with stratified flow. *Nucl. Sci. Engng* **88**, 297–310.

REIMANN, J., JOHN, H. & SEEGER, W. 1981 Transition from slug to annular flow in horizontal air–water and steam–water flow. Report KfK 3189.

SIMPSON, H. C., ROONEY, D. H., GRATTAN, E. & AL-SAMARRAL, F. A. A. 1981 Two-phase flow in large diameter horizontal tubes. NEL Report No. 677.

TAITEL, Y. & DUKLER, E. 1976 A theoretical approach to the Lockhart–Martinelli correlation for stratified flow. *Int. J. Multiphase Flow* **2**, 591–595.

THOM, J. R. S. 1964 Prediction of pressure drop during forced circulation boiling of water. *Int. J. Heat Mass Transfer* **7**, 709–724.

TURNER, J. M. & WALLIS, G. B. 1965 The separate-cylinders model of two-phase flow. Paper No. NYO-3114-6, Thayer's School of Engineering, Dartmouth College, Hanover, N.H.

UEDA, H., MOLLER, R., KOMORI, S. & MIZUSHINA, T. 1977 Eddy diffusivity near the free surface of open channel flow, *Int. J. Heat Mass Transfer* **20**, 1127–1136.

WALLIS, G. B. & DOBSON, J. E. 1973 The onset of slugging in horizontal stratified air–water flow. *Int. J. Multiphase Flow* **1**, 173–193.

ZIVI, S. M. 1963 Estimation of steady-state steam void-fraction by means of the principle of minimum entropy production. *6th natn. Heat Transfer Conf. AIChE-ASME*, Boston, Mass., ASME Preprint 63-HT-16.

ZUBER, N. & FINDLAY, J. A. 1965 Average volumetric concentration in two-phase flow systems. *Trans. ASME J. Heat Transfer* **87C**, 453–468.